Journal of Alloys and Compounds 509 (2011) 7758–7763

Contents lists available at ScienceDirect

Journal of Alloys and Compounds

journal homepage: www.elsevier.com/locate/jallcom

Microstructural and mechanical evaluation of Al–TiB_2 nanostructured composite fabricated by mechanical alloying

Z. Sadeghian [a,*], B. Lotfi [a], M.H. Enayati [b], P. Beiss [c]

[a] Department of Materials Science and Engineering, Faculty of Engineering, Shahid Chamran University, Ahvaz, Iran
[b] Department of Materials Engineering, Isfahan University of Technology, Isfahan 84156-83111, Iran
[c] Institute for Materials Applications in Mechanical Engineering, RWTH Aachen University, Aachen, Germany

ARTICLE INFO

Article history:
Received 17 January 2011
Received in revised form 25 April 2011
Accepted 27 April 2011
Available online 10 May 2011

Keywords:
Aluminum matrix nanocomposite
Mechanical alloying
In situ TiB_2
Spark plasma sintering

ABSTRACT

Production of bulk Al–TiB_2 nanocomposite from mechanically alloyed powder was studied. Al–20 wt.% TiB_2 metal matrix nanocomposite powder was obtained by mechanical alloying (MA) of pure Ti, B and Al powder mixture. A double step process was used to prevent the formation of undesirable phases like Al_3Ti intermetallic compound, which has been described in our previous papers. The resultant powder was consolidated by spark plasma sintering (SPS) followed up by hot extrusion. The structural characteristics of powder particles and sintered samples were studied by X-ray diffractometry (XRD), scanning electron microscopy (SEM) and transmission electron microscopy (TEM). Hardness measurements were conducted on the cross section of powder particles and sintered sample and the tensile behavior of extruded samples was evaluated. The results showed that the prepared Al–20 wt.% TiB_2 nanocomposite has good thermal stability against grain growth and particle coarsening. Extruded Al–20 wt.% TiB_2 showed a hardness value of 180 VHN and yield and tensile strength of 480 and 540 MPa, respectively, which are much higher than those reported for similar composites made by other processes.

1. Introduction

The physical and mechanical properties exhibited by metal matrix composites (MMCs), such as high specific modulus, strength and thermal stability, make them particularly attractive for application in the aerospace and automotive industries [1–4]. Mechanical properties of MMCs can be further enhanced by decreasing the sizes of ceramic particulates and/or matrix grains from micrometer to nanometer level. Such materials are referred to as the nanocomposites [5]. Typical examples are Al-based composites, whose hardness, strength, and Young's modulus can be effectively enhanced when the structure changes to nano scale [6–8]. So far, due to the complexities in the synthesis of metal matrix nanocomposites, systematic investigations on the mechanical properties of these materials and a few reports have been focused on the synthesis of bulk aluminum matrix nanocomposites via powder metallurgy (PM) routes [8]. In situ techniques have been developed to fabricate aluminum-based metal matrix composites (MMCs), in which the reinforcements are synthesized in the matrix during fabrication by chemical reaction of the constituents [9]. The in situ formed reinforcing particles are finer in size and their distribution is more uniform. Furthermore, they are thermodynamically stable in the matrix, leading to less degradation at high temperatures.

The structure and properties of the in situ ceramic phase have been optimized over a variety of processing techniques [9]. These techniques include exothermic dispersion, reactive-gas injection, reactive sintering, reactive milling and mechanical alloying. Mechanical alloying (MA) as a solid state powder processing method has been considered for fabricating in situ MMCs. MA has an advantage over other in situ fabrication routes as it is capable of producing nano structured composite powder with high uniformity.

Even though the in situ composites have significant advantages, some synthesis routes may lead to composites with inhomogeneous microstructure with various unstable and/or undesirable phases [10–12]. These undesirable phases might drastically reduce the mechanical properties. For example, Tjong et al. [13] have investigated the mechanical properties of in situ Al–10 wt.% TiB_2 and found that the formation of Al_3Ti phase has a negative impact on the mechanical performance of in situ composites. They proposed that the elimination of intermetallic Al_3Ti phase is a primary task for developing in situ Al–TiB_2 composites with superior mechanical performance.

A challenge in processing of nanostructured materials is that long time exposure at high temperature sintering, often results in severe grain growth. The consolidation techniques best suited

* Corresponding author at: Department of Materials Science and Engineering, Faculty of Engineering, Shahid Chamran University, Golestan Blvd., Ahvaz, Iran. Tel.: +98 611 3332739; fax: +98 611 3336642.
E-mail address: zsadeghian@yahoo.com (Z. Sadeghian).

0925-8388/$ – see front matter © 2011 Elsevier B.V. All rights reserved.
doi:10.1016/j.jallcom.2011.04.145

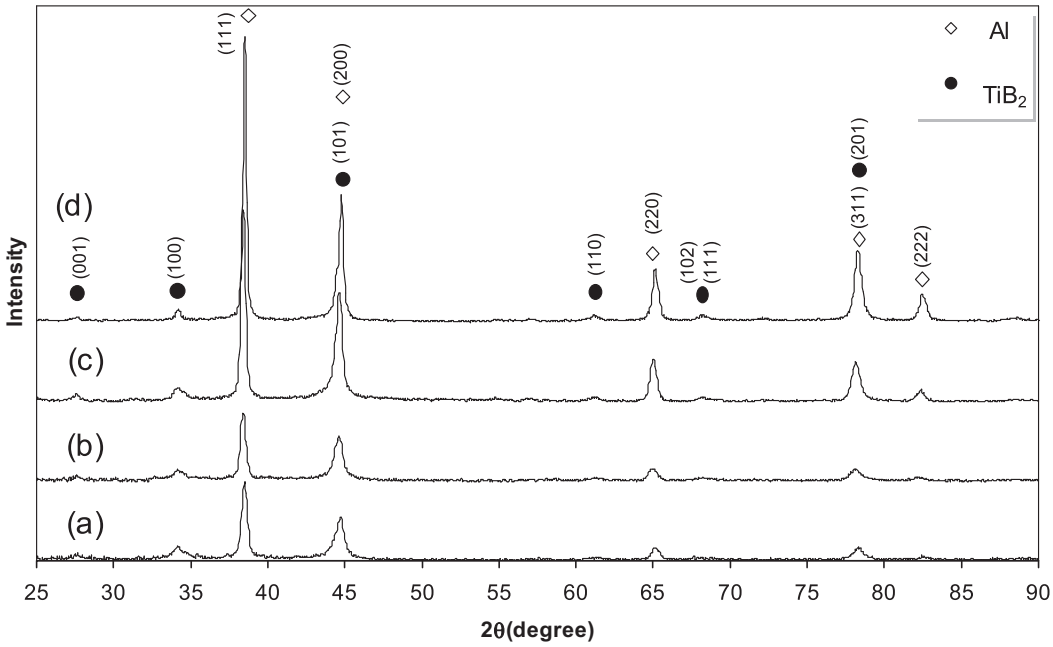

Fig. 1. XRD patterns of Al–20 wt.% TiB_2 nanocomposite (a) as-milled powder obtained from double step MA, (b) after annealing up to 550 °C, (c) SPSed sample and (d) extruded rod.

to retain nanoscale grain size seem to be hot-pressing, hot electric discharge sintering such as plasma activated sintering (PAS), and spark plasma sintering (SPS) that uses microscopic electric discharges between the particles under pressure where, by carefully controlling the processing time, temperature and pressure, it is possible to produce nearly fully dense nanostructured bulk samples [14,15]. According to the literature two attempts have been reported for synthesizing in situ Al–TiB_2 by mechanical alloying, in which Al_3Ti intermetallic compound was also obtained. Furthermore, the resulting powders were not nano-scale and no study has been reported on the mechanical properties of consolidated nanocrystalline Al–TiB_2 composites.

The objective of this study was to synthesize Al–20 wt.% TiB_2 bulk nanostructured composite via several consecutive processing steps including MA, SPS and hot extrusion without the formation of unwanted phases. Microstructure, thermal stability and mechanical properties of extruded samples were also investigated.

2. Materials and methods

Elemental Al 63 μm), Ti (40–60 μm) and B (2 μm) powders were used as starting materials. Powder mixtures were milled by a Fritsch planetary ball mill with a rotating speed of 360 rpm. The ball to powder weight ratio was 10 and the diameter of the chromium steel balls was 15 mm. The hardened chromium steel vial (400 ml) was evacuated and filled with argon to prevent oxidation of powders during the mechanical alloying process. To avoid severe adhesion of aluminum powder to the balls and the vial, 1 wt.% zinc stearate was added to the mixture as a controlling agent. A double step MA process of elemental powders was used to obtain in situ Al–TiB_2 composite powder which is described elsewhere [16,17].

A SEIFERT X-ray diffractometer employing monochromatic Cu K_α radiation (λ = 0.15406 nm) was used to investigate the structural changes during mechanical alloying. XRD scans were performed with a step size of 0.05° and a dwell time per step of 20 s. The cross-sectional microstructure of the powder particles was studied by a LEO scanning electron microscope (SEM). To evaluate the thermal behavior and stability of the powder during subsequent processes, such as sintering, differential scanning calorimetry (DSC) experiments were conducted using Netzsch 402 equipment at heating rate of 15 °C min^{-1} under flowing argon gas. Transmission electron microscopy observations were conducted using a FEI Tecnai G2 TEM instrument working at 200 kV. The TEM samples were prepared by using focused ion beam (FIB) technique.

Powders were sintered by a FCT HP D 250 spark plasma sintering (SPS) machine. The MAed powders were placed inside the graphite die, and the die was placed between the graphite electrodes of the SPS chamber. Argon (99.99% purity) was used as the protecting atmosphere during SPS experiments. The SPS experiments were carried out at DC current of 6000 A and DC voltage of 10 V. Samples were heated up to 550 °C with a constant pressure of 35 MPa, maintained during the heating period and the total time of the process was 600 s. The diameter of the sintered samples was 78 mm. Sintered samples were then hot extruded by backward extrusion in order to obtain suitable rods of Al–TiB_2 composites for mechanical testing. The preheating temperature was 400 °C and the extrusion rate was 0.6 mm s^{-1} with a ratio of 15. Microhardness examination of Al–TiB_2 powders was conducted by a Leco testing machine while the hardness of consolidated samples was measured by a Zwick macrohardness machine. Tensile behavior at ambient temperatures was studied by a Hounsfield H50KS S machine at a strain rate of 0.001 mm s^{-1}.

3. Results and discussion

X-ray examination of the final in situ Al–20 wt.% TiB_2 powder produced by mechanical alloying showed only the presence of TiB_2 in Al matrix and no other phases were observed (Fig. 1a). The grain size of TiB_2 and Al in the powder was estimated by the Williamson–Hall (WH) equation [18]. It was found that both phases had similar grain size of about 20 nm.

According to the dark-field image (Fig. 2b) the average size of the grains was measured to be 20 nm which is in good agreement with the values obtained from the WH equation. By image analysis of SEM image (Fig. 3) it was confirmed that TiB_2 had a nearly uniform distribution in the Al matrix with an average size of about 90 nm.

The DSC trace of powder particles obtained from double step MA process (Fig. 4) represented no exothermic peak up to 550 °C. Furthermore the X-ray diffraction pattern taken after the DSC run remained unchanged compared to that for as-milled powder (Fig. 1b), that reflects the good thermal stability of resulting Al–TiB_2 nanocomposite powder upon heating. The average grain size of TiB_2 did not increase during annealing in DSC, while the grain size of the aluminum matrix grew from about 20 nm to about 30 nm. Therefore the Al–TiB_2 nanocomposite powder was expected to have good thermal stability during subsequent consolidation processes.

The mechanically alloyed Al–TiB_2 powder was sintered using spark plasma sintering (SPS), to cylindrical samples. The density of SPSed sample was measured to be 2.82 g cm^3 which is 96% of the theoretical density of Al–20 wt.% TiB_2 (2.94 g cm^3).

Fig. 1c shows the X-ray diffraction pattern of the SPSed sample compared to the as MAed composite powder. No structural change

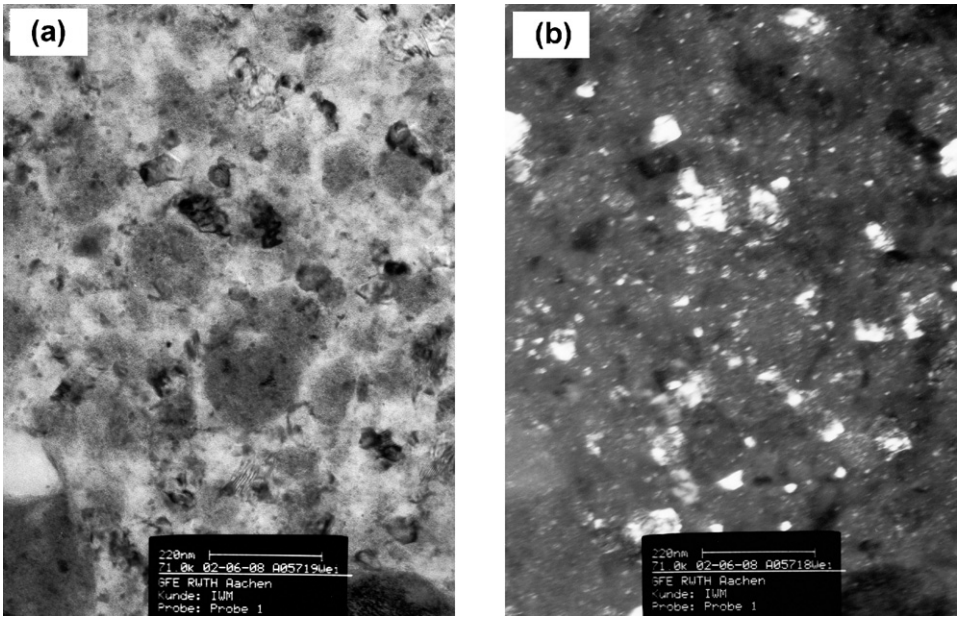

Fig. 2. TEM images of Al–20 wt.% TiB_2 as-milled powder particle obtained from double step MA (a) bright field image, (b) dark field image.

occurred in the Al–TiB_2 nano-composite after consolidation by SPS. The mean grain size of the TiB_2 phase was measured to be about 20 nm. The grain size of the Al matrix for the sintered sample was determined to be about 30 nm which is higher than that for the as-milled powder. Therefore, no significant grain growth occurred in Al during the sintering process. These results showed that the prepared nanocomposite powder has sufficient thermal stability to withstand grain growth during consolidation process. SEM micrograph of the sintered sample is presented in Fig. 5. The maximum size of TiB_2 particles in the sintered sample was measured to be about 3 μm, with a large amount of particles remaining smaller than 100 nm. However, there was still a small amount of porosity of about 3.8% in the SPSed sample.

Hot extrusion was applied on the SPSed billets to eliminate the remaining porosity and produce rods suitable for tensile testing. Radial cracks which progress from the surface towards the centre of the extrudate, known as fir tree defect, has been reported during hot extrusion of Al-based composites [19,20]. This defect occurred during direct hot extrusion attempts in this study, even at an extrusion speed as low as 1 mm s^{-1}. By indirect extrusion at a preheating temperature of 400 °C, extrusion ratio of 15 and extrusion speed of 0.6 mm s^{-1} the billets showed no surface cracking or defects. Fig. 1d shows the diffraction pattern of the extruded sample. The results revealed no structural change in the extruded sample compared to the powder and the sintered sample. This is in agreement with DSC results obtained from MAed powder. The sizes of Al and TiB_2 grains in the extruded sample were measured, using the WH method, to be about 20 and 35 nm, respectively. These results are comparable with those obtained for the powder and the sintered sample. The measured grain size values were confirmed by image analyzing of the TEM dark field image obtained from the extruded sample (Fig. 6b), which showed nano-sized grains with a mean value of about 30 nm.

An SEM micrograph obtained from the cross section of extruded rod is shown in Fig. 7. The size of TiB_2 particles ranged between a few nanometers to about 2 μm. TiB_2 particles showed no

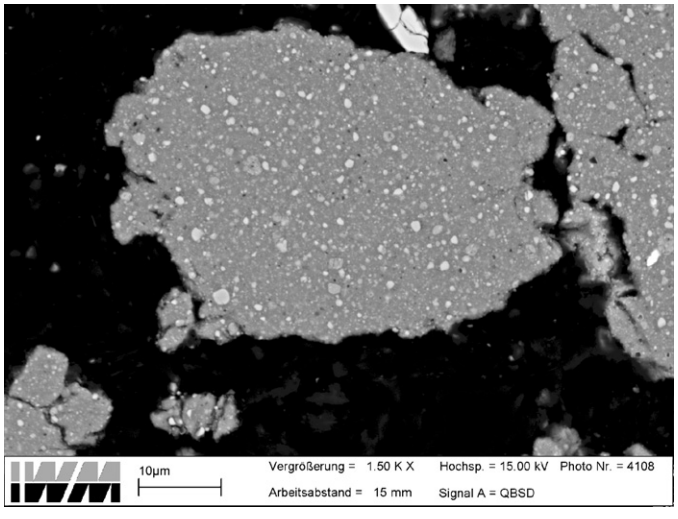

Fig. 3. A typical cross sectional SEM micrograph of Al–20 wt.% TiB_2 as-milled powder particle obtained from double step MA.

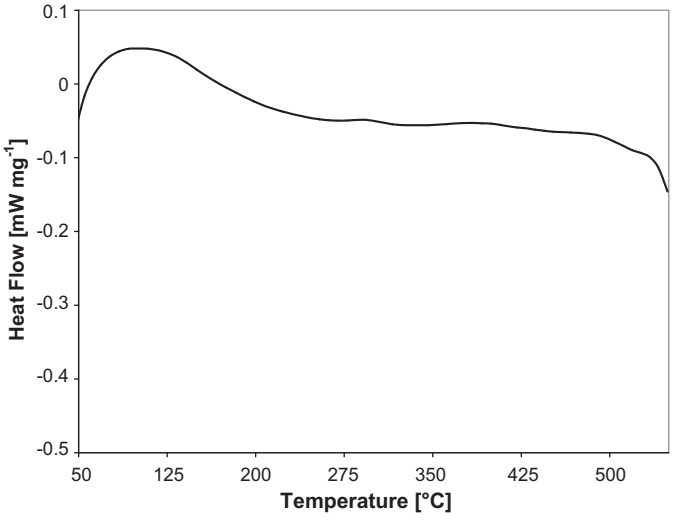

Fig. 4. DSC trace up to 550 °C of the Al–20 wt.% TiB_2 as-milled powder obtained from double step MA.

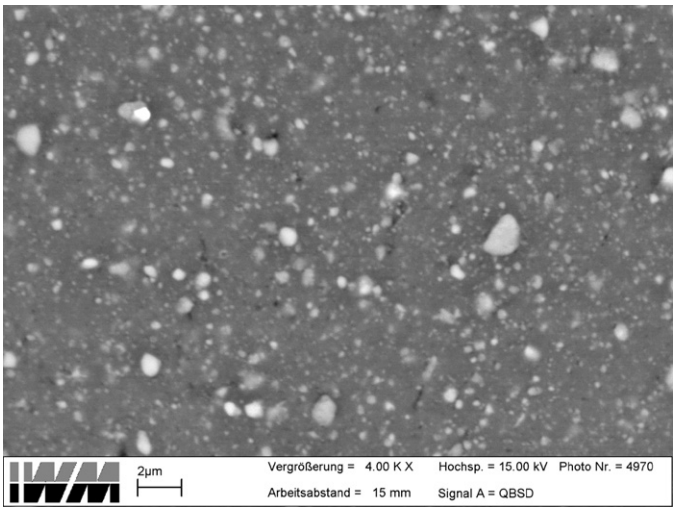

Fig. 5. Cross-sectional SEM micrographs of SPSed Al–20 wt.% TiB_2 sample.

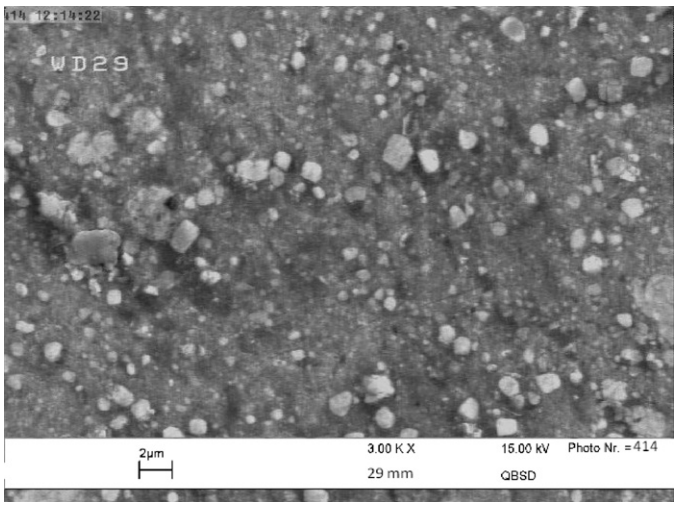

Fig. 7. Cross-sectional SEM micrographs of Al–20 wt.% TiB_2 extruded rod.

Table 1
Hardness values of Al–TiB_2 composites at different stages.

As milled powder (microhardness, VHN)	Sintered sample (hardness, VHN)	Extruded sample (hardness, VHN)
480	206	179

remarkable growth compared to the as-milled powder and the as-sintered sample. TiB_2 is thermodynamically stable in the Al matrix and once formed does not decompose in the matrix [21]. Therefore, dissolution of the particles and diffusion of Ti and B cannot occur during sintering and extrusion processes.

Fig. 8 shows the EFTEM (energy filtered transmission electron microscopy) of the extruded sample. There was no evidence of solved Ti or B in the Al matrix and the distribution of Ti and B was limited to TiB_2 particles. These maps also confirmed that most of TiB_2 particles were smaller than 100 nm.

Table 1 shows the hardness values of Al–20 wt.% TiB_2 at different stages. After consolidation of the powder by SPS the hardness value had decreased by about 50% versus the powder. This can be attributed to the elimination of cold work effects during exposure to high temperatures. The hardness of extruded sample was about 180 HV, which was much higher than those reported previously [11,12]. For example for Al–15 wt.% TiB_2 composite fabricated by mechanical alloying and powder extrusion the hardness was reported to be 84 VHN [11]. Improvement of mechanical properties such as hardness has been stated by other investigators, when the size reduces to nanoscale [22]. It has been shown by Han et al. that reduction of grain size to 200 nm improves the tensile properties of 6061 Al–10 wt.% Al_2O_3 as much as twice [23].

A typical stress–strain curve obtained from the extruded sample is shown in Fig. 9. It is obvious from the curve that Al–TiB_2 nanocomposite shows a brittle behavior in tensile testing. The total elongation of the sample was 1.4%. Tensile properties of extruded Al–20 wt.% TiB_2 nanocomposite produced in this study are presented in Table 2, and Fig. 10 shows the tensile properties of this nanocomposite in comparison with Al–TiB_2 composite reported by other investigators. Both yield strength and tensile strength of extruded Al–TiB_2 nanocomposite of this study are much higher

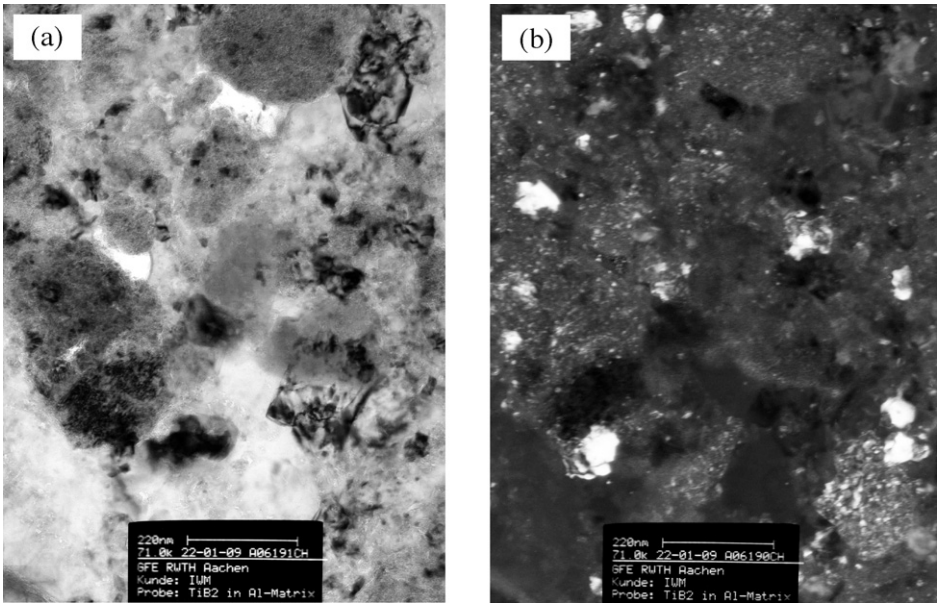

Fig. 6. TEM images of Al–20 wt.% TiB_2 extruded sample (a) bright field image, (b) dark field image.

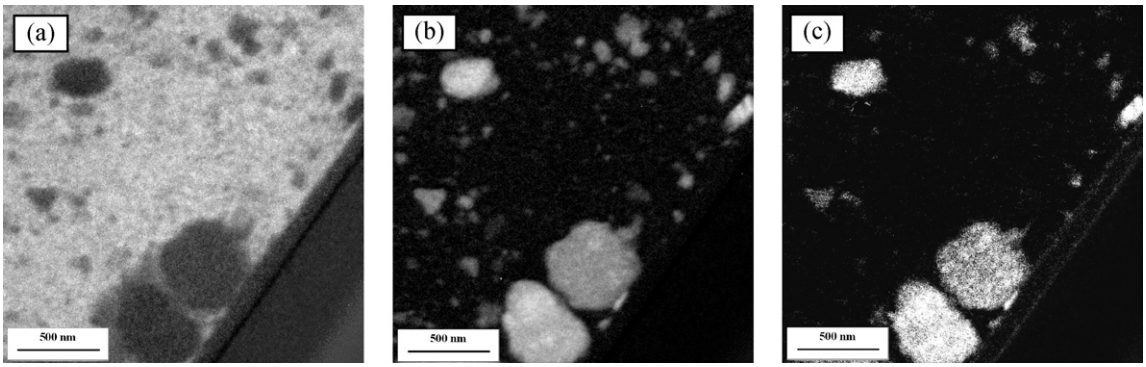

Fig. 8. EFTEM elemental map of Al–20 wt.% TiB_2 extruded rod for (a) Al, (b) Ti and (c) B.

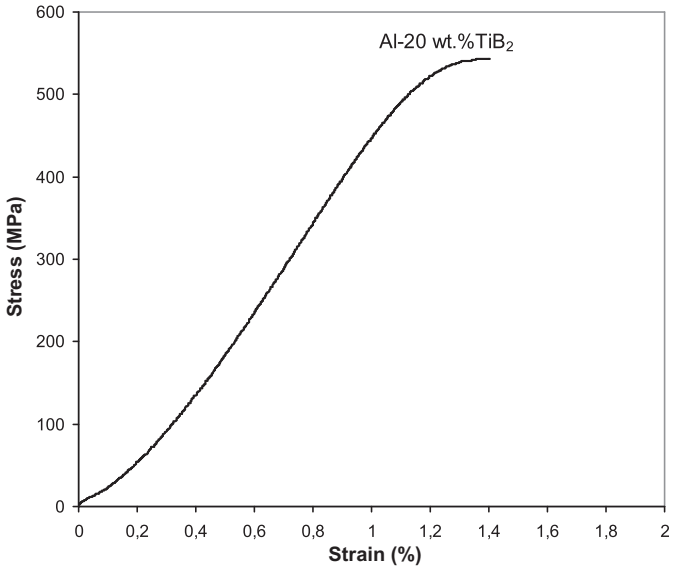

Fig. 9. A typical stress–strain curve obtained from the extruded Al–20 wt.% TiB_2 composite.

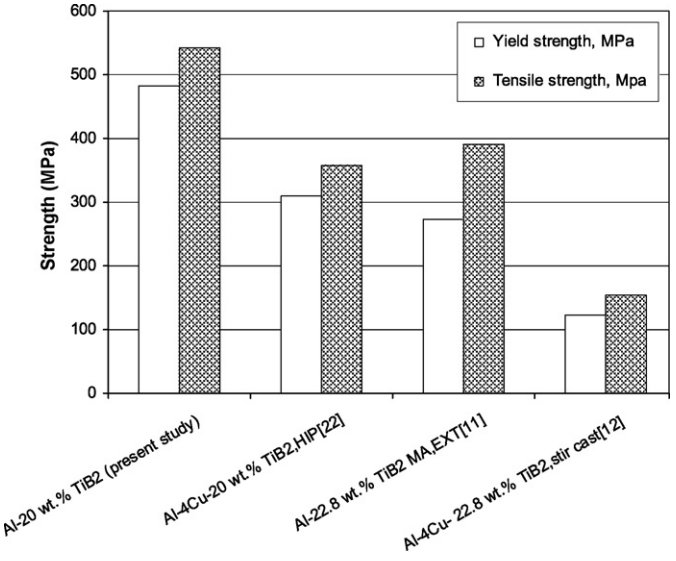

Fig. 10. Tensile properties of some Al–20 wt.% TiB_2 composites prepared by different techniques.

Table 2
Tensile properties of extruded Al–TiB_2 composite.

0.2% proof strength, MPa	Tensile strength, MPa	Elongation, %
483	543	1.4

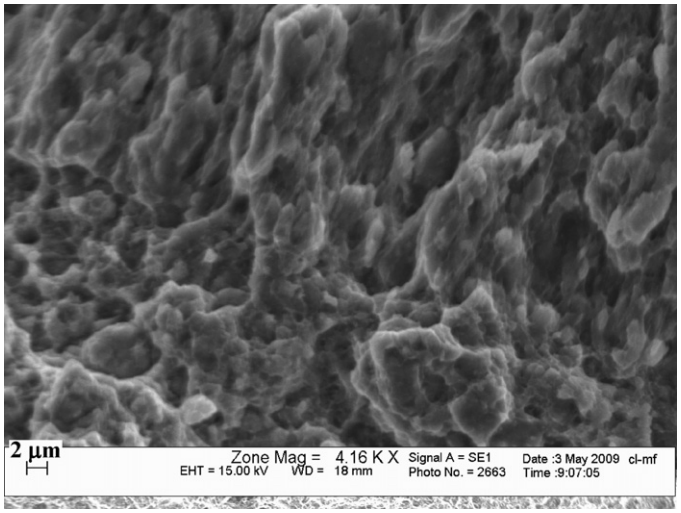

Fig. 11. Fracture surface morphology of extruded Al–20 wt.% TiB_2 composite.

than those reported in previous studies with similar compositions [12,13].

The improved yield strength of the nanocomposite presented here can be explained by an Orowan strengthening mechanism as a result of presence of fine, closely spaced hard particles in the matrix, which hinder the movement of dislocations [24]. It should be noted that the samples fractured with a macroscopically brittle mode, without any evidence of necking. However, fractography of the fractured samples showed that the matrix behaves in a ductile manner at microscopic scale, resulting in the formation of dimples (Fig. 11). Zimmerman et al. and Tang et al. have also reported similar features for the fracture surfaces of Ni–SiC and Al–SiC nanocomposites, previously [25,26].

4. Conclusions

The double step MA process resulted in the in situ formation of TiB_2 particles in the Al matrix with a fine and uniform distribution. The TiB_2 particles size in as-milled Al–20 wt.% TiB_2 powder ranged from 10 nm to 1 μm although most of them were smaller than 100 nm. Hot extrusion did not increase the TiB_2 particle size significantly. The average Al grains in the as-milled powder was measured to be 15 nm which increased to 35 nm after hot extrusion. The

results showed that the prepared Al–20 wt.% TiB_2 nanocomposite has good thermal stability against grain growth and particle coarsening. Extruded Al–20 wt.% TiB_2 nanocomposite showed a hardness value of 180 VHN and yield and tensile strength of 480 and 540 MPa, respectively, which are much higher than those reported for similar composites made by other techniques.

References

[1] J.M. Torralba, C.E. Da Costa, F. Velasco, J. Mater. Process. Technol. 1–2 (2003) 6–203.
[2] Z.Y. Chen, Y.Y. Chen, G.Y. Shu, D. Li, Y.Y. Liu, Metall. Mater. Trans. 31A (2000) 1959–1964.
[3] H. Yi, N. Ma, X. Li, Y. Zhang, H. Wang, Mater. Sci. Eng. A 419 (2006) 12–17.
[4] I.G. Watsona, M.F. Forstera, P.D. Lee, R.J. Dashwood, R.W. Hamilton, A. Chirazi, Composites A 36 (2005) 1177–1187.
[5] S.C. Tjong, Adv. Eng. Mater. 8 (2007) 639–652.
[6] Y.C. Kang, S.L. Chan, Mater. Chem. Phys. 85 (2004) 438–443.
[7] C.J. Hsu, C.Y. Chang, P.W. Kao, N.J. Ho, C.P. Chang, Acta Mater. 549 (2006) 5241–5249.
[8] F. Tang, B.Q. Han, M. Hagiwara, J.M. Schoenung, Adv. Eng. Mater. 9 (2007) 286–291.
[9] S.C. Tjong, Z.Y. Ma, Mater. Sci. Eng. R 29 (2000) 49–113.
[10] l. Lü, H. Lai, Y. Wang, J. Mater. Sci. 35 (2000) 241–248.
[11] L. Lü, M.O. Lai, Y. Su, H.L. Teo, C.F. Feng, Scripta Mater. 45 (2001) 1017–1023.
[12] K.L. Tee, L. Lü, M.O. Lai, Mater. Sci. Technol. 17 (2001) 201–206.
[13] S.C. Tjong, G.S. Wang, Y.M. Mai, Compos. Sci. Technol. 65 (2005) 1537–1546.
[14] V. Viswanathan, Mater. Sci. Eng. R 54 (2006) 121–285.
[15] M. Omori, Mater. Sci. Eng. A 287 (2000) 183–188.
[16] Z. Sadeghian, M.H. Enayati, P. Beiss, Powder Metall. 54 (2011) 46–49.
[17] Z. Sadeghian, M.H. Enayati, P. Beiss, J. Mater. Sci. 44 (2009) 2566–2572.
[18] M.P.C. Kalita, A. Perumal, A. Srinivasan, Mater. Lett. 61 (2007) 824–826.
[19] M. Lieblich, G. Gonzalez-Doncel, P. Adeva, J. Ibañez, M. Torralba, G. Caruana, J. Mater. Sci. Lett. 16 (1997) 726–728.
[20] R.K. Goswami, R. Sikand, A. Dhar, O.P. Grover, U.C. Jindal, A.K. Gupta, Mater. Sci. Technol. 15 (1999) 443–449.
[21] I. Gotman, Mater. Sci. Eng. A 187 (1994) 189–195.
[22] Y.Q. Liu, H.T. Cong, W. Wang, C.H. Sun, H.M. Cheng, Mater. Sci. Eng. A 505 (2009) 151–156.
[23] B. Han, T. Langdon, Mater. Sci. Eng. A 410–411 (2005) 430–434.
[24] Z. Zhang, D.L. Chen, Mater. Sci. Eng. A 483–484 (2008) 148–152.
[25] A.F. Zimmerman, G. Palumbo, K.T. Aust, U. Erb, Mater. Sci. Eng. A 328 (2002) 137–146.
[26] F. Tang, M. Hagiwara, J.M. Schoenung, Mater. Sci. Eng. A 407 (2005) 306–314.